Measurement of the Dalitz plot slopes of the $K^{\pm} \to \pi^{\pm}\pi^{+}\pi^{-}$ decay

The NA48/2 Collaboration

J.R. Batley, A.J. Culling, G. Kalmus, C. Lazzeroni, D.J. Munday, M.W. Slater, S.A. Wotton

Cavendish Laboratory, University of Cambridge, Cambridge, CB3 0HE, U.K. [1]

R. Arcidiacono, G. Bocquet, N. Cabibbo, A. Ceccucci, D. Cundy [2], V. Falaleev, M. Fidecaro, L. Gatignon, A. Gonidec, W. Kubischta, A. Norton, A. Maier, M. Patel, A. Peters

CERN, CH-1211 Genève 23, Switzerland

S. Balev, P.L. Frabetti, E. Goudzovski [3], P. Hristov [4], V. Kekelidze, V. Kozhuharov, L. Litov, D. Madigozhin, E. Marinova, N. Molokanova, I. Polenkevich, Yu. Potrebenikov, S. Stoynev, A. Zinchenko

Joint Institute for Nuclear Research, 141980 Dubna, Russian Federation

E. Monnier [5], E. Swallow, R. Winston

The Enrico Fermi Institute, The University of Chicago, Chicago, Illinois, 60126, U.S.A.

P. Rubin, A. Walker

Department of Physics and Astronomy, University of Edinburgh, JCMB King's Buildings, Mayfield Road, Edinburgh, EH9 3JZ, U.K.

W. Baldini, A. Cotta Ramusino, P. Dalpiaz, C. Damiani, M. Fiorini, A. Gianoli, M. Martini, F. Petrucci, M. Savrié, M. Scarpa, H. Wahl

Dipartimento di Fisica dell'Università e Sezione dell'INFN di Ferrara, I-44100 Ferrara, Italy

A. Bizzeti [6], M. Calvetti, E. Celeghini, E. Iacopini, M. Lenti, F. Martelli [7], G. Ruggiero [4], M. Veltri [7]

Dipartimento di Fisica dell'Università e Sezione dell'INFN di Firenze, I-50125 Firenze, Italy

M. Behler, K. Eppard, K. Kleinknecht, P. Marouelli, L. Masetti, U. Moosbrugger, C. Morales Morales, B. Renk, M. Wache, R. Wanke, A. Winhart

Institut für Physik, Universität Mainz, D-55099 Mainz, Germany [8]

D. Coward [9], A. Dabrowski, T. Fonseca Martin [4], M. Shieh, M. Szleper, M. Velasco, M.D. Wood [10]

Department of Physics and Astronomy, Northwestern University, Evanston Illinois 60208-3112, U.S.A.

G. Anzivino, P. Cenci, E. Imbergamo, A. Nappi, M. Pepe, M.C. Petrucci, M. Piccini, M. Raggi, M. Valdata-Nappi

Dipartimento di Fisica dell'Università e Sezione dell'INFN di Perugia, I-06100 Perugia, Italy

C. Cerri, G. Collazuol, F. Costantini, L. DiLella, N. Doble, R. Fantechi, L. Fiorini, S. Giudici, G. Lamanna, I. Mannelli, A. Michetti, G. Pierazzini, M. Sozzi

Dipartimento di Fisica dell'Università, Scuola Normale Superiore e Sezione dell'INFN di Pisa, I-56100 Pisa, Italy

B. Bloch-Devaux, C. Cheshkov [4], J.B. Chèze, M. De Beer, J. Derré, G. Marel, E. Mazzucato, B. Peyaud, B. Vallage

DSM/DAPNIA - CEA Saclay, F-91191 Gif-sur-Yvette, France

M. Holder, M. Ziolkowski

Fachbereich Physik, Universität Siegen, D-57068 Siegen, Germany[11]

S. Bifani, C. Biino, N. Cartiglia, M. Clemencic[4], S. Goy Lopez, F. Marchetto

Dipartimento di Fisica Sperimentale dell'Università e Sezione dell'INFN di Torino, I-10125 Torino, Italy

H. Dibon, M. Jeitler, M. Markytan, I. Mikulec, G. Neuhofer, L. Widhalm

Österreichische Akademie der Wissenschaften, Institut für Hochenergiephysik, A-10560 Wien, Austria[12]

To be submitted to Physics Letters B.

Abstract

The distribution of the $K^{\pm} \to \pi^{\pm}\pi^{+}\pi^{-}$ decays in the Dalitz plot has been measured by the NA48/2 experiment at the CERN SPS with a sample of 4.71×10^{8} fully reconstructed events. With the standard Particle Data Group parameterization the following values of the slope parameters were obtained: $g = (-21.134 \pm 0.014)\%$, $h = (1.848 \pm 0.039)\%$, $k = (-0.463 \pm 0.012)\%$. The quality and statistical accuracy of the data have allowed an improvement in precision by more than an order of magnitude, and are such as to warrant a more elaborate theoretical treatment, including pion-pion rescattering, which is in preparation.

[1]Funded by the U.K. Particle Physics and Astronomy Research Council

[2]Present address: Istituto di Cosmogeofisica del CNR di Torino, I-10133 Torino, Italy

[3]Present address: Scuola Normale Superiore, I-56100 Pisa, Italy

[4]Present address: CERN, CH-1211 Genève 23, Switzerland

[5]Also at Centre de Physique des Particules de Marseille, IN2P3-CNRS, Université de la Méditerranée, Marseille, France

[6]Also Istituto di Fisica, Università di Modena, I-41100 Modena, Italy

[7]Istituto di Fisica, Università di Urbino, I-61029 Urbino, Italy

[8]Funded by the German Federal Minister for Education and research under contract 05HK1UM1/1

[9]Permanent address: SLAC, Stanford University, Menlo Park, CA 94025, U.S.A.

[10]Present address: UCLA, Los Angeles, CA 90024, U.S.A.

[11]Funded by the German Federal Minister for Research and Technology (BMBF) under contract 056SI74

[12]Funded by the Austrian Ministry for Traffic and Research under the contract GZ 616.360/2-IV GZ 616.363/2-VIII, and by the Fonds für Wissenschaft und Forschung FWF Nr. P08929-PHY

Introduction

The $K^\pm \to \pi^\pm\pi^+\pi^-$ decay can be described [1] in terms of the Lorentz invariant kinematic variables u and v defined as

$$u = \frac{s_3 - s_0}{m_\pi^2}, \quad v = \frac{s_2 - s_1}{m_\pi^2}; \quad s_i = (P_K - P_i)^2, \; i = 1,2,3; \quad s_0 = \frac{s_1 + s_2 + s_3}{3}. \tag{1}$$

Here m_π is the charged pion mass, P_K and P_i are the kaon and pion four-momenta, the indices $i = 1, 2$ correspond to the two pions of the same electric charge ("even" pions), and the index $i = 3$ to the other ("odd") pion. The experimental Dalitz plot distribution of the $K^\pm \to \pi^\pm\pi^+\pi^-$ decay has been up to now experimentally analyzed [2, 3] in terms of a polynomial expansion in powers of u and v:

$$|M(u,v)|^2 \sim C(u,v) \cdot (1 + gu + hu^2 + kv^2). \tag{2}$$

Here g, h, k are the linear and quadratic slope parameters (terms proportional to odd powers of v are forbidden by Bose symmetry, and the variable v is defined only up to a sign), and $C(u,v)$ is the Coulomb factor [4]:

$$C(u,v) = \prod_{i,j=1,2,3;\; i<j} \{n_{ij}/(e^{n_{ij}} - 1)\}, \quad n_{ij} = 2\pi\alpha q_i q_j/\beta_{ij}, \tag{3}$$

where $q_i = \pm 1$ are the pion charges, α is the fine structure constant, and β_{ij} is the relative velocity of the pions i and j, expressed via the squared invariant mass of the pion pair s_{ij} as

$$\beta_{ij} = \left(1 - \frac{4m_\pi^2}{s_{ij}}\right)^{1/2} \left(1 - \frac{2m_\pi^2}{s_{ij}}\right)^{-1}. \tag{4}$$

Among the measurements of the slope parameters performed in the past, the most precise are reported in [2] based on 1.5×10^6 $K^\pm$ decays, and in [3] based on 0.225×10^6 K^+ decays.

The primary goal of the NA48/2 experiment at CERN SPS is the search for direct CP-violating charge asymmetries of Dalitz plot linear slopes in $K^\pm \to \pi^\pm\pi^+\pi^-$ [5] and $K^\pm \to \pi^\pm\pi^0\pi^0$ [6] decays. However, the large data sample collected also allows a study of the Dalitz plot distributions to be performed at a new level of precision, estimating the detector acceptance with a detailed Monte Carlo (MC) simulation.

The parameterization (2) of the $K^\pm \to \pi^\pm\pi^+\pi^-$ decay distribution takes into account electromagnetic interactions only in the first approximation [4] and totally neglects pion rescattering effects [7, 8], which were recently shown by NA48/2 to contribute significantly to the distribution of $K^\pm \to \pi^\pm\pi^0\pi^0$ decays [9]. The current study aims to measure the Dalitz plot slopes within the conventional framework (2), and represents a first step towards a more complete description of the decay distribution. In particular, the presence of radiative effects and strong final state interactions, both ignored in the current work, imply that the slope parameters obtained, while fully comparable to those defined in the Particle Data Group compilation [1], should not be attributed any precise physical significance as far as the parameterization of the weak decay in terms of more fundamental parameters is concerned; this would require an improved theoretical framework which is just being developed [8], and its implementation is postponed for a forthcoming analysis.

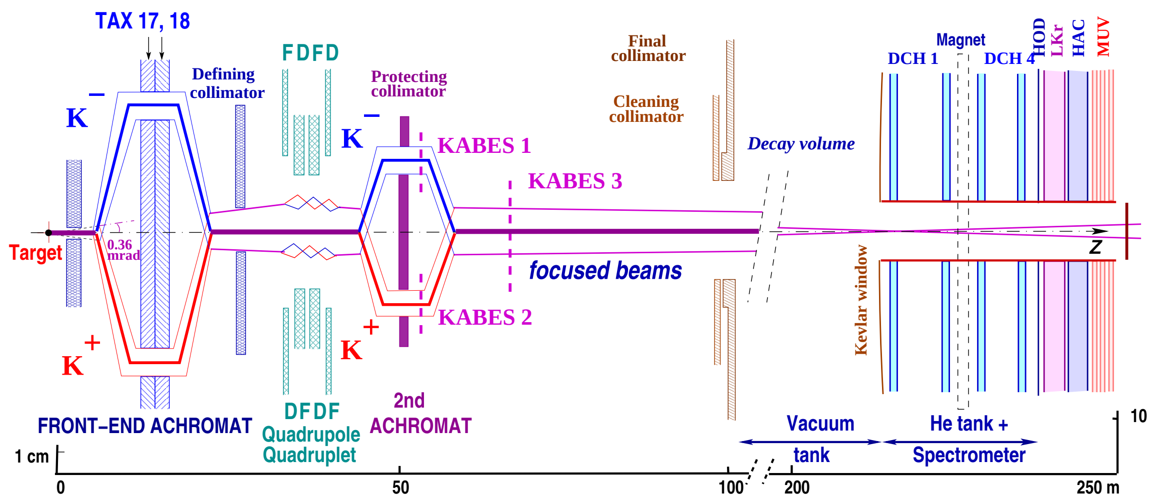

Figure 1: Schematic lateral view of the NA48/2 beam line (TAX17,18: motorized beam dump/collimators used to select the momentum of the K^+ and K^- beams; FDFD/DFDF: focusing set of quadrupoles, KABES1–3: kaon beam spectrometer stations), decay volume and detector (DCH1–4: drift chambers, HOD: hodoscope, LKr: EM calorimeter, HAC: hadron calorimeter, MUV: muon veto). Note that the vertical scales are different in the two parts of the figure.

NA48/2 collected data during two runs in 2003 and 2004, with about 50 days of efficient data taking in each run. This analysis is based on 4.71×10^8 fully reconstructed $K^\pm \to \pi^\pm\pi^+\pi^-$ events, corresponding to 55% of the data sample collected during the NA48/2 run of 2003.

1 Beams and detectors

A beam line providing two simultaneous charged beams of opposite signs overlapping in space all along the decay volume was designed and built in the high intensity hall (ECN3) at the CERN SPS. The beam line is a key element of the experiment, as it allows decays of K^+ and K^- to be recorded at the same time, and therefore leads to cancellation of several systematic uncertainties for the charge asymmetry measurement. Regular alternation of magnetic fields in all the beam line elements was adopted. The layout of the beams and detectors is shown schematically in Fig. 1. The setup is described in a right-handed orthogonal coordinate system with the z axis directed downstream along the beam, and the y axis directed vertically up.

The beams are produced by 400 GeV/c protons impinging at zero incidence angle on a beryllium target of 40 cm length and 2 mm diameter. Charged particles with momentum (60 ± 3) GeV/c are selected in a charge-symmetric way by an achromatic system of four dipole magnets with zero total deflection (‘achromat’), which splits the two beams in the vertical plane and then recombines them on a common axis. Then the beams pass through a defining collimator and a series of four quadrupoles designed to produce focusing of the beams towards the detector. Finally the two beams are again split in the vertical plane and recombined in a second achromat, where three stations of a Micromega-type [10] detector form a kaon beam spectrometer [11] (not used in the present analysis).

After passing the cleaning and the final collimators, the beams enter the decay volume housed in a 114 m long cylindrical vacuum tank with a diameter of 1.92 m for the first 65 m, and 2.4 m for the rest. Both beams follow the same path in the decay volume: their axes coincide within 1 mm, while the transverse size of the beams is about 1 cm. With 7×10^{11} protons incident on the target per burst of ~ 4.8 s duration, the positive (negative) beam flux at the entrance of the decay volume is 3.8×10^7 (2.6×10^7) particles per pulse, of which 5.7% (4.9%) are K^+ (K^-). The K^+/K^- flux ratio is about 1.8. The fraction of beam kaons decaying in the decay volume at nominal momentum is 22%.

The decay volume is followed by a magnetic spectrometer used for reconstructing $K^\pm \to \pi^\pm\pi^+\pi^-$ decays. The spectrometer is housed in a tank filled with helium at nearly atmospheric pressure, separated from the vacuum tank by a thin ($0.31\%X_0$) Kevlar composite window. A thin-walled aluminium beam pipe of 16 cm outer diameter traversing the centre of the spectrometer (and all the following detectors) allows the undecayed beam particles and the muon halo from decays of beam pions to continue their path in vacuum. The spectrometer consists of four drift chambers (DCH): DCH1, DCH2 located upstream, and DCH3, DCH4 downstream of a dipole magnet. The magnet has a field integral $\int B_y dz = 0.4$ Tm, thus providing a horizontal transverse momentum kick $\Delta P_x = 120$ MeV/c for charged particles. The DCHs have the shape of a regular octagon with a transverse size of about 2.8 m and a fiducial area of about 4.5 m^2. Each chamber is composed of eight planes of sense wires arranged in four pairs of staggered planes oriented horizontally, vertically, and along each of the two orthogonal 45° directions. The spatial resolution of each DCH is $\sigma_x = \sigma_y = 90\mu$m. The nominal momentum resolution of the magnetic spectrometer is parameterized as $\sigma_p/p = (1.02 \oplus 0.044 \cdot p)\%$ (p expressed in GeV/c). The measured resolution on the reconstructed $3\pi^\pm$ invariant mass varied during the running period corresponding to the considered data sample in the range of $(1.65 - 1.72)$ MeV/c^2, depending on DCH performance.

The magnetic spectrometer is followed by a plastic scintillator hodoscope (HOD) used to produce fast trigger signals and to provide precise time measurements of charged particles. The hodoscope has a regular octagonal shape with a transverse size of about 2.4 m. It consists of a plane of horizontal and a plane of vertical strip-shaped counters. Each plane consists of 64 counters arranged in four quadrants. Counter widths (lengths) vary from 6.5 cm (121 cm) for central counters to 9.9 cm (60 cm) for peripheral ones.

The hodoscope is followed by a liquid krypton electromagnetic calorimeter (LKr), a hadronic calorimeter (HAC) and a muon detector (MUV), all of which are not used in the present analysis. A detailed description of the components of the NA48 detector can be found elsewhere [12].

The $K^\pm \to \pi^\pm\pi^+\pi^-$ events are triggered with a two-level system. At the first level (L1), the rate of ~ 500 kHz is reduced to ~ 100 kHz by requiring coincidences of hits in the two planes and in at least two of the 16 segments of the HOD. The second level (L2) is based on a hardware system computing coordinates of hits from DCH drift times, and a farm of asynchronous microprocessors performing fast reconstruction of tracks and running a selection algorithm, which requires at least two tracks to originate in the decay volume with the closest distance of approach below 5 cm. L1 triggers not satisfying this condition are examined further and accepted nevertheless if there is a reconstructed track which is not kinematically compatible with a $\pi^\pm\pi^0$ decay of a $K^\pm$ having momentum of 60 GeV/c directed along the beam axis. The resulting trigger rate is about 10 kHz.

2 Data analysis

Reconstruction and selection

Event reconstruction is based entirely on the magnetic spectrometer information. Tracks are reconstructed from hits in DCHs using the measured magnetic field map rescaled according to the recorded value of electric current in the spectrometer analyzing magnet. Three-track vertices, compatible with a $K^\pm \to \pi^\pm\pi^+\pi^-$ decay, are reconstructed by extrapolation of track segments from the upstream part of the spectrometer back into the decay volume, taking into account the stray magnetic fields due to the Earth's field and parasitic magnetization of the vacuum tank, and multiple scattering in the Kevlar window. The stray field correction is based on a three-dimensional field map measured in the entire vacuum tank, and reduces the amplitude of the observed sinusoidal variation of the reconstructed 3π invariant mass on the azimuthal orientation of the odd pion by more than an order of magnitude to a level below 0.05 MeV/c^2. The event kinematics is calculated using measured momenta and track directions extrapolated to the decay vertex.

The principal selection criteria applied to the reconstructed variables are the following:

- Total charge of the three pion candidates: $Q = \pm 1$;
- Transverse momentum: $P_T < 0.3$ GeV/c;
- Longitudinal vertex position within the decay volume: $Z_{vtx} > Z_{final\ coll.}$;
- Transverse vertex radius within the beam area: $R_{vtx} < 3$ cm;
- Kaon momentum within the nominal range: 54 GeV/$c < |\vec{P}_K| <$ 66 GeV/c.

To improve the resolution on the kinematic variables, and to reduce the impact of differences between data and MC resolutions, the events were passed through a kinematic fitting procedure with three constraints (constraining the initial kaon direction to by along the z axis, and the 3π invariant mass to the kaon mass). Events with the quality of the kinematic fit corresponding to probability $p < 10^{-5}$ were rejected. The fraction of these rejected events increases as a function of deviation of the reconstructed 3π mass from the kaon nominal mass $|\Delta M|$; in particular, all the events with $|\Delta M| > 10$ MeV/c^2 were rejected by the above condition.

The geometric acceptance for the $K^\pm \to \pi^\pm\pi^+\pi^-$ decays is mainly determined by the beam pipe traversing the centres of the DCHs, and the material in the central region of each DCH where central DCH wires terminate. This material defines a region of high DCH inefficiency[1]. This inefficiency together with beam optics performance and variations influences the acceptance, and is difficult to reproduce accurately with a MC simulation. To minimize the effects of this problem, it is required that the transverse positions of each pion in DCH1 and DCH4 planes $\vec{R}_{\pi i}$ ($i = 1, 4$) satisfy the condition $|\vec{R}_{\pi i} - \vec{R}_0| > 18$ cm, where $\vec{R}_0$ is the position of the momentum-weighted average of the three pions' impact points: $\vec{R}_0 = \sum_{i=1}^{3}(\vec{R}_{\pi i}|\vec{P}_{\pi i}|)/\sum_{i=1}^{3}|\vec{P}_{\pi i}|$ (for DCH4 plane, trajectories of pions are extrapolated from upstream the magnet). $\vec{R}_0$ corresponds to the transverse

[1] The acceptance is not biased by the finite outer size of the DCHs due to a relatively small Q-value of the $K^\pm \to \pi^\pm\pi^+\pi^-$ decay: $Q = 75.0$ MeV.

position of the line of flight of the initial kaon. The value of 18 cm was chosen to exclude safely the inefficient central region taking into account the beam sizes and variations of their average transverse positions. The described selection criterion costs about 50% of the statistics; however an appropriate MC description of the experimental conditions is more important than the sample size for the present analysis[2].

The selection leaves a sample of 4.71×10^8 events, which is practically background free, as $K^\pm \to \pi^\pm\pi^+\pi^-$ is by far the dominant decay mode of the charged kaon with more than one charged particle in the final state. The fact that backgrounds due to other decays of beam kaons and pions are negligible was also checked with a MC simulation.

The distribution of the reconstructed $3\pi^\pm$ invariant mass of data events (before the kinematic fitting) and its comparison with MC are presented in Fig. 2a. The non-Gaussian tails of the mass distribution are primarily due to $\pi^\pm \to \mu^\pm\nu_\mu$ decays in flight, and are well understood in terms of MC simulation. The ratio of MC to data mass spectra is presented in Fig. 2b. It demonstrates imperfection of resolution description in MC, and a deficit of MC events in the low mass region, which however contains a small fraction of the events, and is mostly outside the signal region. The Dalitz plot distribution of the selected data events (after the kinematic fitting) used for the subsequent analysis is presented in Fig. 2c. The bin sizes of the Dalitz plot distributions used in the analysis are $\delta u = \delta v = 0.05$.

Correction for trigger inefficiency

To simplify the treatment of the trigger inefficiency, stable trigger performance was the main condition used to select the sample to be used for the analysis[3]. Inefficiencies of both L1 and L2 trigger components were directly measured as functions of $(u, |v|)$ using control data samples of prescaled low bias triggers collected along with the main triggers, which allowed to correct the observed $(u, |v|)$ distributions, and propagate the statistical errors of trigger inefficiencies into the result.

The L1 trigger condition requiring a coincidence of hits in two of the 16 non-overlapping HOD segments is loose, as there are three charged particles in a fully reconstructed event, providing a rather low (and stable in time) inefficiency of 0.6×10^{-3} for the selected event sample. However, the L1 inefficiency depends rather strongly on the kinematic variables. The primary mechanism generating such a dependence is the enhancement of inefficiency for topologies with two pions hitting the same HOD segment; such events preferably belong to the kinematic regions characterized by small relative velocity of a certain $\pi\pi$ pair in the kaon rest frame.

The L2 inefficiency, which is due to local DCH inefficiencies, which affect the trigger more strongly than the off-line reconstruction due to lower redundancy and trigger timing effects, was measured to be $(0.32 \pm 0.05) \times 10^{-2}$ (the error indicates the maximum size of its variation during the data taking period). It did not exhibit any significant correlation to the kinematic variables, due to relative complexity of the decision taking algorithm.

Monte Carlo simulation

A detailed GEANT-based MC simulation was developed, which includes full detector geometry and material description, simulation of stray magnetic fields, DCH local inef-

[2]In a different case, the charge asymmetry analysis [5] is performed with soft cuts maximizing the selected data sample, and is based on cancellation, rather than simulation, of the systematic effects.

[3]As it was already noted, the size of the data sample is not a limitation for this analysis.

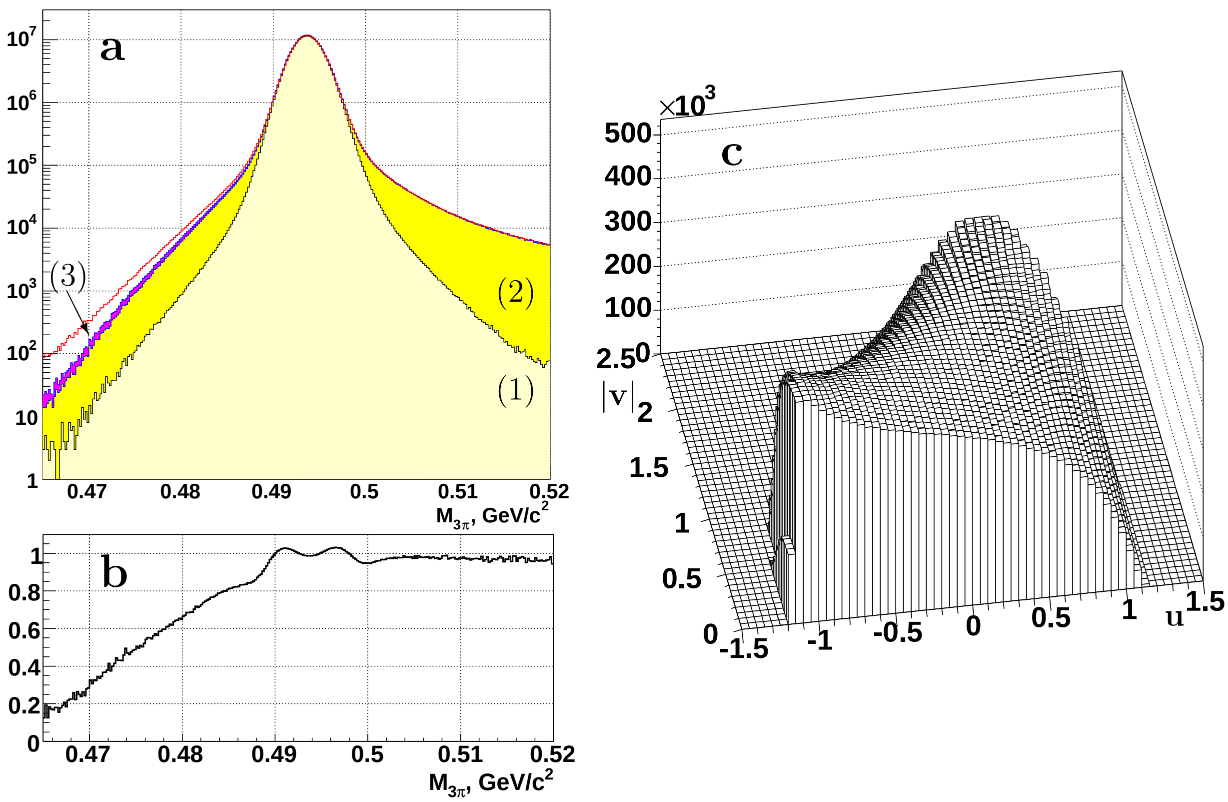

Figure 2: (a) Reconstructed spectrum of $3\pi^{\pm}$ invariant mass $M(3\pi)$ (upper line) and its presentation in terms of normalized MC components: (1) events without $\pi \to \mu\nu$ decay in flight, (2) events with $\pi \to \mu\nu$ decay, (3) IB radiative $K_{3\pi\gamma}$ events. (b) The ratio of MC/data $M(3\pi)$ spectra demonstrating imperfection of resolution description in MC, and a deficit of MC events at low $M(3\pi)$ outside the signal region. (c) Reconstructed distribution in the kinematic variables $F_{data}(u, |v|)$ (after kinematic fit).

ficiencies and misalignment, the beam line (which allows to reproduce kaon momentum spectra and beam profiles), and K^+/K^- relative fluxes. Moreover, time variations of the above effects during the running period were simulated. A production of 6.7×10^9 $K^{\pm} \to \pi^{\pm}\pi^{+}\pi^{-}$ events distributed according to the matrix element (2) with PDG values of the slope parameters [1] was performed to determine the detector acceptance. A sample of 1.16×10^9 MC events (almost 2.5 times larger than the data sample) passes the selection.

Comparison of data and MC distributions in such significant variables as longitudinal vertex position and illuminations of DCH1 and DCH4 planes by pions is presented in Fig. 3, and demonstrates that MC simulation reproduces the data distributions to a level of a few units of 10^{-3}.

Fitting procedure

The measurement method is based on fitting of the binned reconstructed data distribution $F_{data}(u, |v|)$ presented in Fig. 2c with a sum of four reconstructed MC components generated according to the four terms in the polynomial (2) presented in Fig. 4. Let us denote these reconstructed MC distributions as $F_0(u, |v|)$, $F_u(u, |v|)$, $F_{u^2}(u, |v|)$, and $F_{v^2}(u, |v|)$. To obtain them, the MC sample (produced with a single fixed distribution) was divided

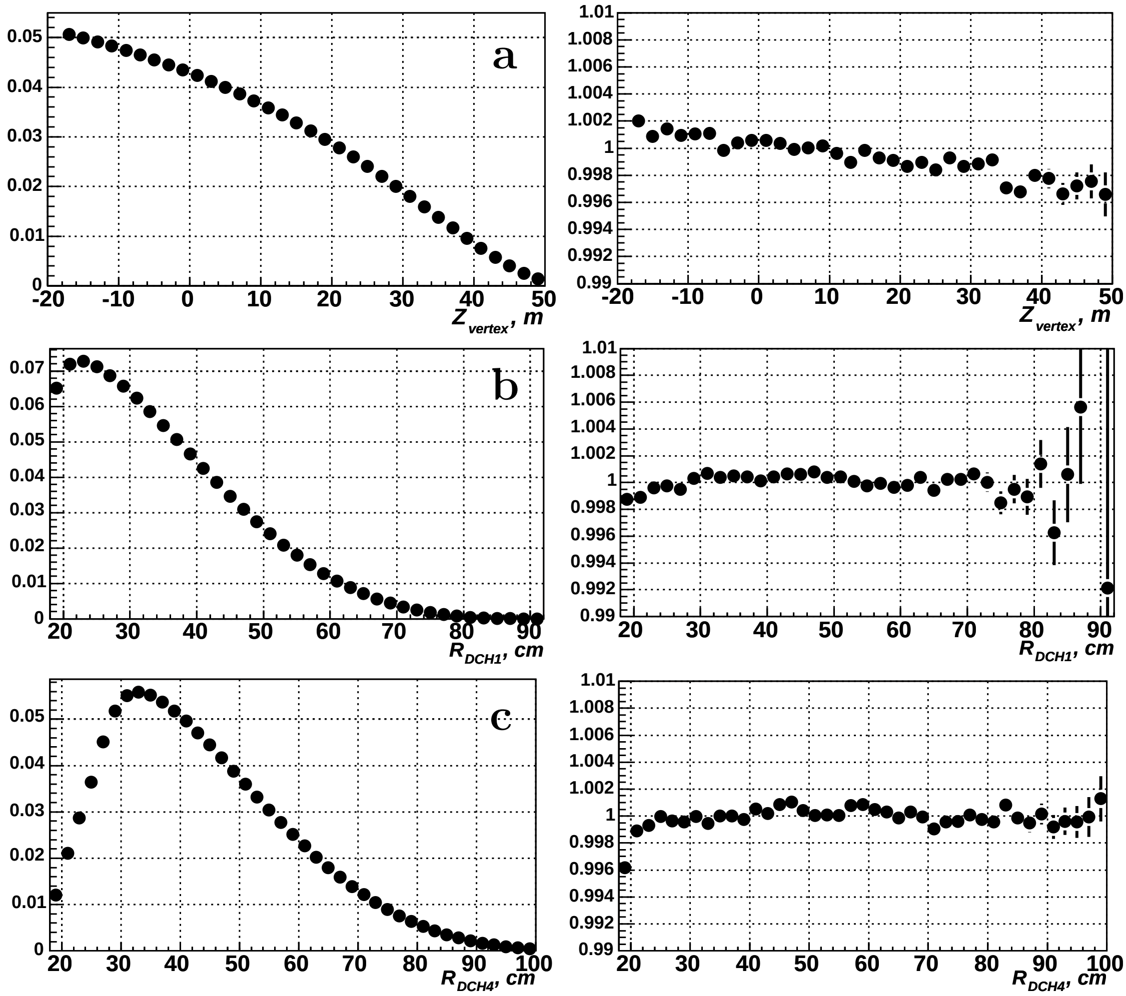

Figure 3: Left column: reconstructed data distributions, right column: the corresponding ratios of data/MC distributions of (a) vertex z position; pion distance (for each of the 3 pions) from the z axis in the planes of (b) DCH1 and (c) DCH4.

into four subsamples[4], and events in each subsample were assigned appropriate weights depending on the generated $(u, |v|)$ to obtain the desired distributions.

The following functional defining the agreement of the shapes of data and MC distributions is minimized using the MINUIT package [13] in order to measure the values of the slope parameters (g, h, k):

$$\chi^2(g,h,k,N) = \sum_{u,|v|\ \text{bins}} \frac{(F_{data}(u,|v|) - NF_{MC}(g,h,k,u,|v|))^2}{\delta^2 F_{data}(u,|v|) + N^2\delta^2 F_{MC}(g,h,k,u,|v|)}. \quad (5)$$

The sum is evaluated over all the bins of reconstructed $(u, |v|)$ distributions with at least 1000 data events, which allows to avoid non-Gaussian behaviour of errors. Here $\delta F_{data}(u, |v|)$ is an uncertainty of the number of data events in a given bin (composed of a statistical part and a trigger efficiency part added in quadrature), $F_{MC}(g, h, k, u, |v|)$ is

[4]The relative sizes of the four subsamples were subject of optimization in order to minimize the statistical error of the measurement.

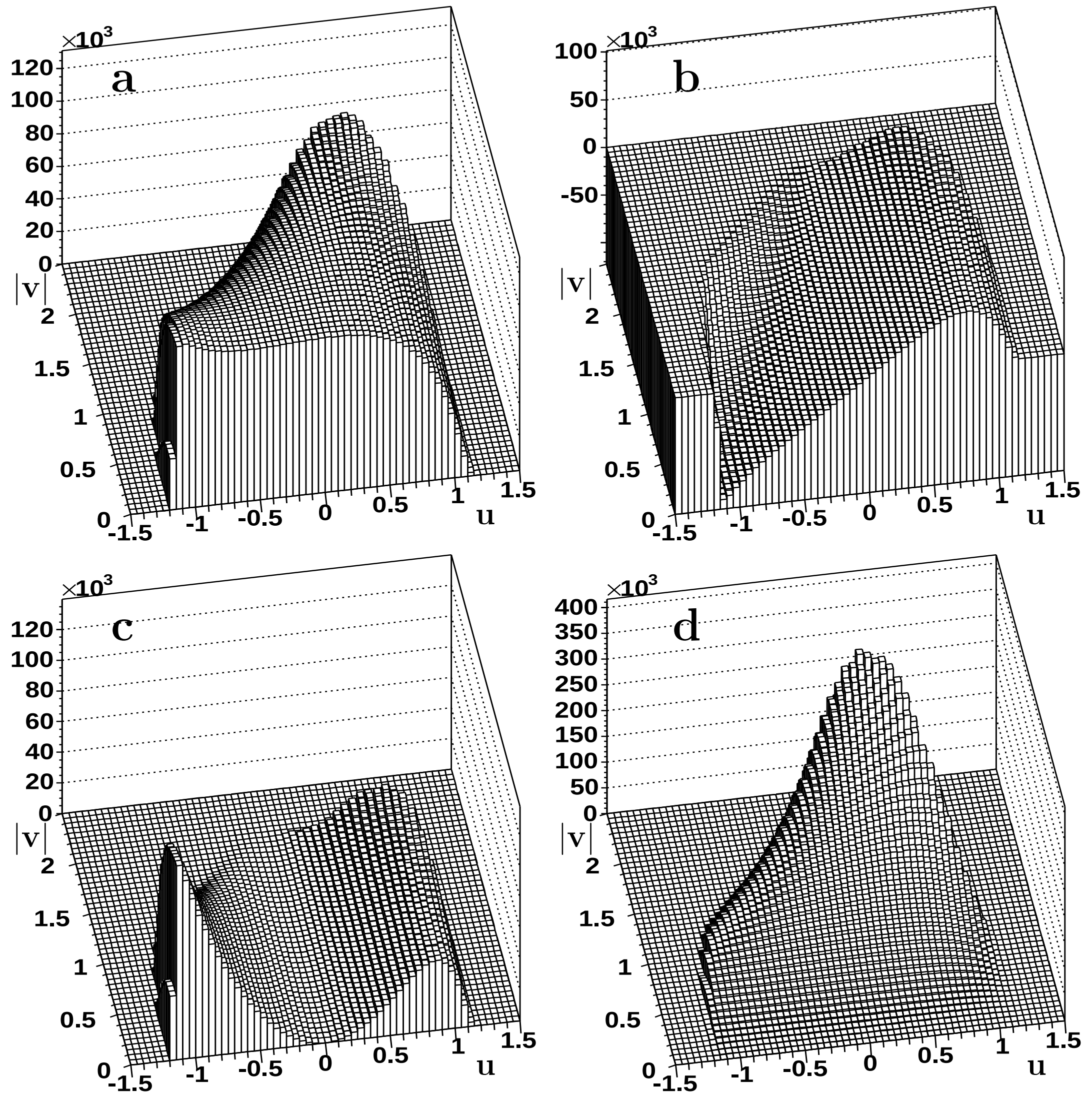

Figure 4: Reconstructed distributions in the kinematic variables $(u,|v|)$ of the four MC components: (a) $F_0(u,|v|)$, (b) $F_u(u,|v|)$, (c) $F_{u^2}(u,|v|)$, (d) $F_{v^2}(u,|v|)$.

a MC population of a bin for given values of (g,h,k):

$$F_{MC}(g,h,k,u,|v|) = F_0(u,|v|)/I_0 + gF_u(u,|v|)/I_u + hF_{u^2}(u,|v|)/I_{u^2} + kF_{v^2}(u,|v|)/I_{v^2}, \tag{6}$$

and $\delta F_{MC}(g,h,k,u,|v|)$ is its statistical error:

$$\delta^2 F_{MC}(g,h,k,u,|v|) = \delta^2 F_0(u,|v|)/I_0^2 + g^2\delta^2 F_u(u,|v|)/I_u^2 + h^2\delta^2 F_{u^2}(u,|v|)/I_{u^2}^2 + k^2\delta^2 F_{v^2}(u,|v|)/I_{v^2}^2. \tag{7}$$

Here I_0, I_u, I_{u^2} and I_{v^2} are the normalization constants computed by taking into account the numbers of generated events in each of the four MC subsamples, and the integrals of the four terms in (2) over the Dalitz plot. The free parameters of the functional (5) are the slope parameters (g,h,k) and an overall MC normalization parameter N.

The minimization yields $\chi^2/\mathrm{NDF} = 1669/1585$, corresponding to a satisfactory probability of 7.0%. The results of the fit and the trigger corrections are presented in Table 1.

Parameter	Value	Uncertainties		Trigger correction
		statistical	MC stat.	
$g \times 10^2$	-21.134 ± 0.013	0.009	0.008	-0.008 ± 0.005
$h \times 10^2$	1.848 ± 0.022	0.015	0.013	0.116 ± 0.009
$k \times 10^2$	-0.463 ± 0.007	0.005	0.004	0.033 ± 0.003

Table 1: Fit results with statistical and MC statistical uncertainties, trigger corrections and their statistical uncertainties. The trigger corrections are included into the resulting values.

The non-zero values of the corrections arise mostly from the L1 trigger inefficiency dependence on kinematic variables, while their statistical errors receive contributions of similar sizes from L1 and L2 trigger efficiency uncertainties.

Keeping only the linear term gu in (2) yields a fit of unacceptable quality: $\chi^2/\mathrm{NDF} = 13683/1583$. Including the terms proportional to u^3 and uv^2 (the only cubic terms allowed by Bose symmetry) yields values for the corresponding cubic slope parameters compatible with zero.

Stability checks

Stability of the results with respect to variations of the selection conditions on vertex quality, P_T, R_{vtx}, $\vec{R}_{\pi i}$ and $|\vec{P}_K|$, binning variation, with respect to exclusion of $(u, |v|)$ bins with large deviations of the Coulomb factor (3) from unity, and with respect to kaon sign[5] were checked. No statistically significant dependencies were found. Stability with respect to various ways of binning the data was checked; comparison of slope measurements in bins of reconstructed longitudinal coordinate of decay vertex Z_{vtx} (since the acceptance depends strongly on this variable), and in data taking periods are shown in Fig. 5 as the most significant examples.

Systematic uncertainties

The main source of systematic uncertainty is the imperfect description of the resolution in pion momentum, which can be observed in Fig. 2b as a slight disagreement of the shapes of the reconstructed $M(3\pi)$ spectra for data and MC. To evaluate the corresponding effect, two different plausible ways of introducing smearing of the MC resolution were used: increasing the smearing of DCH space points from 90μm to 100μm, and adding an extra $0.09\% X_0$ layer of matter in the position of the Kevlar window. The sizes of the added perturbations are such to correct for the concavity of the ratio presented in Fig. 2b. The resulting uncertainties are listed in Table 2.

The measurement of pion momenta is based on the knowledge of the magnetic field in the spectrometer magnet. The variation of the magnet current can be monitored with a relative precision of 5×10^{-4}. Smaller variations are continuously controlled with a precision of $\sim 10^{-5}$ by the deviation of the measured charge-averaged kaon mass from the nominal value. A time-dependent correction is introduced by scaling the reconstructed pion momenta, decreasing the effect of overall field scale to a negligible level. To account for possible differences between the shape of the field map used for simulation and the

[5] Combined K^+ and K^- sample is used to obtain the result. Stability of the slope paremeters with respect to kaon sign is a consequence of the experimental fact [5] that CP invariance holds at the discussed level of precision.

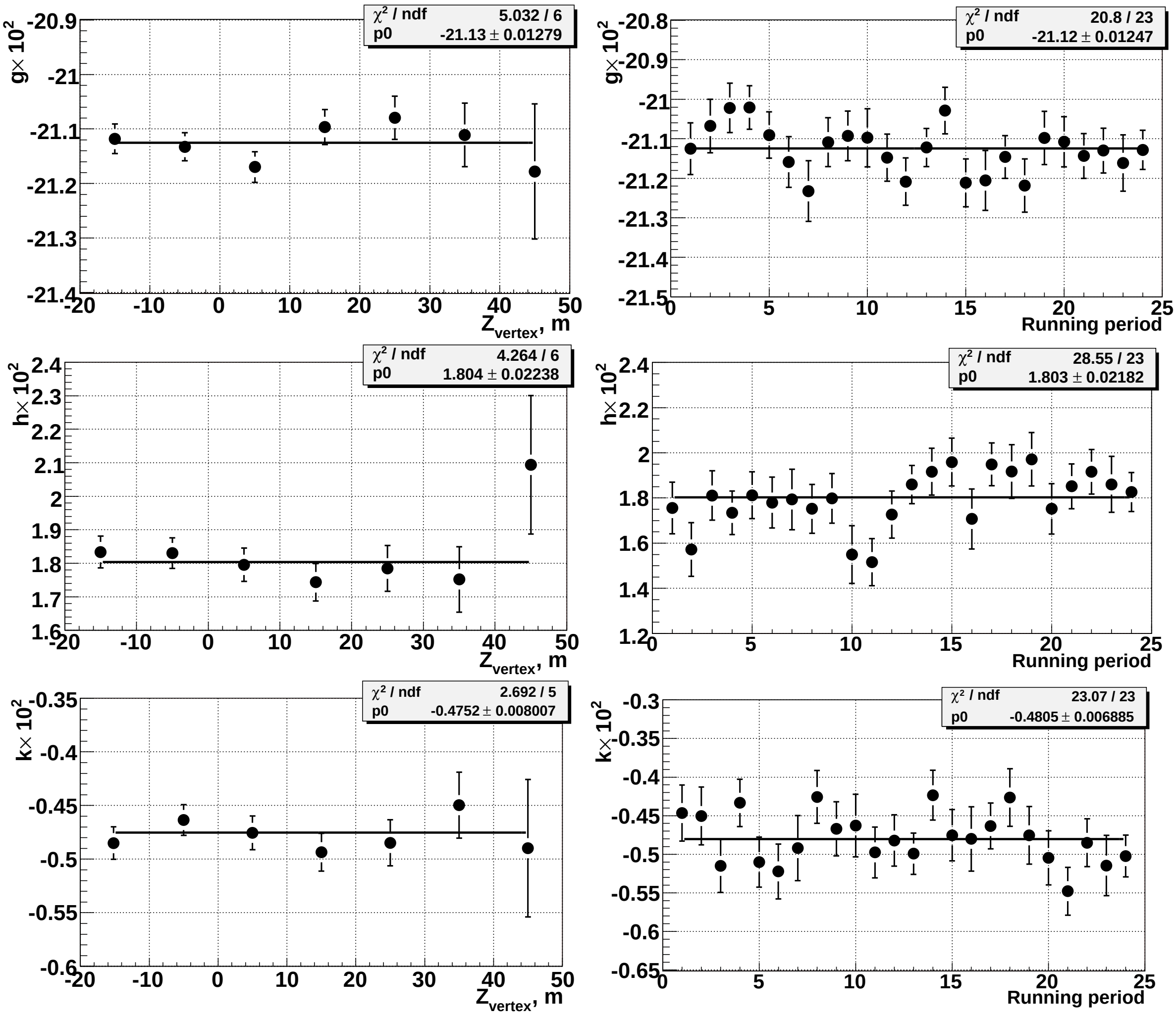

Figure 5: Slope measurements in bins of Z_{vtx} (left column) and in running periods (right column). Systematic errors are not shown.

true field, variations of the MC field map were artificially introduced, consistently with the known precision of field measurement of $\sim 10^{-3}$. The corresponding uncertainties are listed in Table 2.

The transverse positions of DCHs and individual wires were controlled and realigned at the level of reconstruction software every 2–4 weeks of data taking using data collected in special runs in which muon tracks were recorded with no magnetic field in the spectrometer. This allows an alignment precision of ~ 30 μm to be reached. However, time variations of DCH alignment on a shorter time scale can bias the measurement. These variations were measured by the difference between the average reconstructed 3π invariant masses for K^+ and K^- decays, and taken into account. The precision with which these effects are simulated leads to systematic uncertainties presented in Table 2.

The effects due to limited precision of measurement of the stray magnetic field in the decay volume were estimated by variation of the stray field map used for decay vertex reconstruction; the corresponding systematic effects are presented in Table 2.

The kaon momentum spectra were carefully simulated, and the related residual uncertainties are negligible. Possible differences between data and MC transverse scales were

Effect	$\delta g \times 10^2$	$\delta h \times 10^2$	$\delta k \times 10^2$
Pion momentum resolution	0.004	0.031	0.009
Spectrometer magnetic field	0.002	0.008	0.004
Spectrometer misalignment	0.002	0.002	0.001
Stray magnetic field	0.001	0.002	0.001
Total	0.005	0.032	0.010

Table 2: A summary of the systematic uncertainties.

found to have a negligible influence on the result.

The total systematic errors were obtained by summing the above contributions in quadrature, and are presented in Table 2.

Conclusions

The results on the Dalitz plot slope parameters in $K^\pm \to \pi^\pm\pi^+\pi^-$ decays obtained with a fraction of NA48/2 data sample, ignoring radiative effects (apart from the Coulomb factor) and strong rescattering effects, are

$$g = (-21.134 \pm 0.014)\%, \quad h = (1.848 \pm 0.039)\%, \quad k = (-0.463 \pm 0.012)\%.$$

These values are in agreement with the world averages [1], and have an order of magnitude smaller uncertainties. This is the first measurement of a non-zero value of the quadratic slope parameter h. The compatibility of the measured distribution with the PDG polynomial parameterization [1] appears to be still acceptable at an improved level of precision; no significant higher order slope parameters were found.

The whole NA48/2 sample suitable for $K^\pm \to 3\pi^\pm$ Dalitz plot shape analysis contains at least three times more data; a more elaborate analysis is foreseen when the corresponding theoretical framework is available.

References

[1] W.-M. Yao *et al.* (PDG), J. Phys. **G33** (2006) 1.

[2] W.T. Ford *et al.*, Phys. Lett. **B38** (1972) 335.

[3] B. Devaux *et al.*, Nucl. Phys. **B126** (1977) 11.

[4] A.A. Bel'kov *et al.*, hep-ph/9311295.

[5] J.R. Batley *et al.* (NA48/2), Phys. Lett. **B634** (2006) 474.

[6] J.R. Batley *et al.* (NA48/2), Phys. Lett. **B638** (2006) 22.

[7] N. Cabibbo and G. Isidori, JHEP **0503** (2005) 021.

[8] G. Colangelo *et al.*, Phys. Lett. **B638** (2006) 187.

[9] J.R. Batley *et al.* (NA48/2), Phys. Lett. **B633** (2006) 173.

[10] Y. Giomataris *et al.*, Nucl. Instr. Methods **A376** (1996) 29.

[11] B. Peyaud *et al.*, Nucl. Instr. Methods **A535** (2004) 247.

[12] V. Fanti *et al.* (NA48), NIMA-D-07-00056 (2007).

[13] F. James and M. Roos, Comp. Phys. Comm. **10** (1975) 343.